



Enhanced nutrient removal from lake water via biodegradation of poly (L-lactide)/poly (3-hydroxybutyrate-co-4-hydroxybutyrate) blends

| | |
|-------------------------------|--|
| Journal: | <i>RSC Advances</i> |
| Manuscript ID | RA-ART-09-2015-019501.R1 |
| Article Type: | Paper |
| Date Submitted by the Author: | 09-Dec-2015 |
| Complete List of Authors: | MAI, JINGJING; Tongji University, chai, xiaoli; Tongji University, Su, Lianghu; Nanjing Institute of Environmental Sciences of the Ministry of Environmental Protection, Li, Qiang; Tongji University, Zhao, Xin; Tongji University, |
| Subject area & keyword: | Nanoscience - Environmental < Environmental |
| | |



Enhanced nutrient removal from lake water via biodegradation of poly (L-lactide)/poly (3-hydroxybutyrate-co-4-hydroxybutyrate) blends

Received 00th January 20xx,
Accepted 00th January 20xx

DOI: 10.1039/x0xx00000x

www.rsc.org/

J. J. Mai,^a X. L. Chai,*^a L. H. Su,^b Q. Li^a and X. Zhao^a

Shaped insoluble PLA/P(3HB-co-4HB) blends were applied as slow-release carbon sources to promote the removal of nutrients and facilitate the control of eutrophication in lake water. Various weight ratios of PLA/P(3HB-co-4HB) blends were prepared by electrospinning and melt compounding processes and were added to static aerated lake water. The properties of the blends and nutrient removal from lake water were characterized. The results demonstrated that nutrient removal was enhanced by degradation of PLA/P(3HB-co-4HB) blends, and the consumption of degradation products further promoted the degradation of blends. The orthophosphate concentrations of water samples with electrospun and melt compounded blends exhibited decreases of 59.3% - 86.4% and 77.8% - 92.6%, respectively, within 12 hours and decreased to approximately zero over time. Ammonium was completely removed within 1.5 - 6.5 days and 2.5 - 5.5 days from water samples with electrospun and melt compounded blends, respectively. Inhibition of nitrite accumulation was observed, and the total inorganic nitrogen content decreased by 9.1% - 49.5% and 19.8% - 52.9% within 8 days in water samples with electrospun and melt compounded blends, respectively. Thus, PLA/P(3HB-co-4HB) blends are potentially useful as slow-release carbon sources for nutrient removal from lake water. Moreover, Fourier transform infrared spectroscopy (FTIR), wide-range X-ray diffraction (XRD) and scanning electron microscopy (SEM) were used to characterize the degradation of PLA/P(3HB-co-4HB) blends, and the results showed that the degradation of PLA/P(3HB-co-4HB) blends is closely related to the crystallinity, surface morphology and composition of blends. Given the blends' favorable properties and high efficiency of nutrient removal, PLA/P(3HB-co-4HB) blends are potentially useful as slow-release carbon sources for nutrient removal from lake water. Melt compounded blends with 50 wt-% PLA are considered to be the optimal choice for this application.

1. Introduction

Eutrophic water with a high nitrogen and phosphorus content promotes the proliferation of algae, which results in serious environmental problems and endangers the health of humans and animals. Ideally, control of eutrophication should be effective and low-cost without generating secondary pollution, while simultaneously maintaining the ecological balance of the lake. Ecological restoration is superior to physical-chemical processes¹. Aquatic ecological regulation and restoration such as phytoremediation with *Phragmites australis*, *Eichhornia crassipes* and *Alopecurus pratensis*²⁻⁵, is environmentally friendly but time-consuming. Hence, novel ecological approaches are needed to control eutrophication, and a feasible option is to control eutrophication by removing nutrients from lake water. Supplied with carbon sources, nitrogen and phosphorus can be removed via the metabolism of microorganisms. Liquid carbon sources without slow-release

characteristics have been widely applied to enhance the denitrification reaction, but they typically lead to secondary pollution by organics; thus, insoluble biopolyesters have a potential application in eutrophication control.

Biodegradable polyesters have attracted attention due to their biorenewable nature, biocompatibility, biodegradability, mechanical properties and potential for environmentally friendly applications⁶⁻¹¹. Fabrication methods such as electrospinning¹²⁻¹⁴, melt compounding^{15,16}, solvent casting^{7,17} and selective polymer extraction¹⁶ have been introduced to facilitate these applications. Many studies have focused on the environmental degradation of biodegradable polyesters in reservoirs¹⁸, marine environments¹⁹⁻²¹, soil²² and compost²³. Poly (lactic acid) (PLA) and poly (3-hydroxybutyrate-co-4-hydroxybutyrate) (P(3HB-co-4HB)) are two biodegradable polyesters that can be degraded in the natural environment.

PLA is synthesized via either chemical processes²⁴ or microbial processes²⁵. PLA is a promising biodegradable polyester with high mechanical strength, biocompatibility^{24,26} and low cost, but it possesses low biodegradability. P(3HB-co-4HB) is produced via the microbial processes of such organisms as *Ralstonia eutropha*, *Pseudomonas oleovorans* and *Chromatium vinosum*²⁷. P(3HB-co-4HB) exhibits low

^a State Key Laboratory of Pollution Control and Resource Reuse, Tongji University, Shanghai 200092, China. Email: xlchai@tongji.edu.cn

^b Nanjing Institute of Environmental Sciences of the Ministry of Environmental Protection, Nanjing 210046, China

mechanical strength, poor thermal stability, and it is expensive to produce, but it is highly biodegradable. Therefore, blending PLA and P(3HB-co-4HB) could improve the mechanical strength and biodegradability of these materials for the control of eutrophication.

Previous study²⁶ has revealed that the degradation of PLA in biological environment occurs in two main stages: hydrolysis and enzymolysis. Water diffuses into the bulk polymer during the hydrolytic step, leading to random non-enzymatic cleavage of ester linkages. The low molecular products are then assimilated by fungi and bacteria, a process which only takes place on the surface of the polyesters. Research on the degradation of P(3HB-co-4HB) has shown that P(3HB-co-4HB) is degraded by microbial-catalyzed erosion from the surface to the interior²², and the molecular weights of samples remain almost unchanged during the course of biodegradation. It has also been found that the degradation of P(3HB-co-4HB) correlates strongly with the crystallinity and surface morphology of the biopolyester²⁸.

Different blends of PLA and P(3HB-co-4HB) biodegrade at different rates because PLA and P(3HB-co-4HB) are degraded by different mechanisms. P(3HB-co-4HB) is reported to degrade at a more rapid rate than PLA. Research on the ratios of melt compounded PLA/P(3HB-co-4HB) blends has demonstrated that the biodegradability of PLA/P(3HB-co-4HB) blends in soil is negatively correlated with PLA content²². Moreover, researchers have investigated the porous materials resulting from selective enzymatic degradation of PLA/P(3HB-co-4HB) blends that were prepared using a melt compounding process with different ratios of PLA and P(3HB-co-4HB). The results revealed that the enzymolysis of PLA/P(3HB-co-4HB) blends is related to blending ratios, and the enzymolysis rates of PLA and P(3HB-co-4HB) are improved in the presence of the other compound because of increases in the specific surface area of the blends¹⁶. Biodegradable PLA/P(3HB-co-4HB) blends with an optimal blending ratio have the potential for innovative application as slow-release carbon sources for nutrient removal.

In this study, various ratios of PLA/P(3HB-co-4HB) blends were prepared via electrospinning and melt compounding processes. The degradation of PLA/P(3HB-co-4HB) blends and the removal of nutrients from eutrophic water were investigated. Fourier transform infrared spectroscopy, wide-range X-ray diffraction and scanning electron microscopy were used to characterize the functional groups, crystallinity and morphology of blends and to clarify the degradation mechanism of PLA and P(3HB-co-4HB) in eutrophic lake water.

2. Materials and Methods

2.1 Materials

Poly (lactic acid) (PLA) was purchased from NatureWorks LLC (USA). The number-average molar mass, as determined by gel permeation chromatography (GPC), was $M_n = 134000$ g/mol,

with a polydispersity $M_w/M_n = 1.99$. Poly (3-hydroxybutyrate-co-4-hydroxybutyrate) (P(3HB-co-4HB)) was purchased from GreenBio (Tianjin, China) with a number-average molar mass $M_n = 680000$ g/mol and a polydispersity $M_w/M_n = 1.96$, as revealed by GPC. The monomer composition of poly(3HB-co-4HB) was 84.6% 3-HB units and 15.4% 4-HB units according to ¹H NMR. Dichloromethane (DCM) and N, N-dimethylformamide (DMF) were purchased from SCRC LLC (Shanghai, China). PLA and P(3HB-co-4HB) were vacuum-dried overnight prior to use. All other materials were used as received.

2.2 Synthesis of PLA/P(3HB-co-4HB) blends

2.2.1 Electrospinning of PLA/P(3HB-co-4HB) blends. Two-component solutions of PLA/P(3HB-co-4HB) blends were prepared for electrospinning by mixing an 8% (w/v) P(3HB-co-4HB) solution and a 12% (w/v) PLA solution. The P(3HB-co-4HB) solution was prepared at room temperature by dissolving 8 g P(3HB-co-4HB) in 100 mL DCM. The PLA solution was prepared at room temperature by dissolving 12 g PLA in 100 mL of an organic solvent mixture containing (7:3, v/v) DCM and DMF. The resulting solutions were stirred overnight. In this manner, a homogeneous, viscous and spinnable solution was obtained. The P(3HB-co-4HB) and PLA solutions were then mixed in different weight ratios (100:0, 70:30, 50:50, 30:700 and 0:100) for electrospinning. The spinnable feed solution was poured into a plastic syringe equipped with a stainless steel needle, which was connected to a high-voltage DC supplier. During the electrospinning process, the feed solution was pressurized at a rate of 0.7 mL/h using a trace injection device. The voltage applied was 17 ± 0.5 kV, and the distance between the needle and the aluminum foil collector was 18 cm. The electrospinning process was conducted at ambient temperature and less than 40% humidity; the spun nanofibers were dried under vacuum for 24 h to remove any residual organic solution.

2.2.2 Melt compounding of PLA/P(3HB-co-4HB) blends.

PLA/P(3HB-co-4HB) blends were mixed in a series of weight ratios (100:0, 70:30, 50:50, 30:700 and 0:100), which were prepared in a Haake batch internal mixer (Haake Rheomix 600, Karlsruhe, Germany) with a batch volume of 50 mL. The melt compounding was performed at 180 °C and a screw speed of 50 rpm during a total mixing time of 8 min, until the viscosity had reached a nearly constant value. After mixing, all the samples were cut into small pieces and hot-pressed at 180 °C for 3 min followed by a cold-press at room temperature to form sheets. The compression molding steps were conducted carefully to ensure that every sample received identical treatment.

2.3 Characterization and biodegradation assays of PLA/P(3HB-co-4HB) blends

2.3.1 FT-IR spectroscopy. The composition of synthesized blends before and after degradation was assessed with FT-IR spectroscopy using a Bruker Tensor 37 (Bruker, Germany). Spectra were collected at room temperature in attenuated total reflection (ATR) mode with a resolution of 4 cm^{-1} (128 scans). A background spectrum was obtained prior to each test to compensate for the effect of humidity and the presence of carbon dioxide; these were removed by spectral subtraction.

2.3.2 X-ray diffraction. The crystallinity of synthesized blends before and after degradation was assessed using a Bruker D8 advance diffractometer (Bruker, Germany). Samples were tested across the range of $5\text{--}40^\circ$ with a scan speed of 0.4. The $\text{Cu K}\alpha$ radiation ($\lambda = 0.15418\text{ nm}$) source was operated at 40 kV and 200 mA. The crystallinity of the blends was estimated using MID JADE 6.5 software.

2.3.4 Biodegradation assays in lake water. Two batch tests were conducted with electrospun PLA/P(3HB-co-4HB) blends and melt compounded PLA/P(3HB-co-4HB) blends (batch test I and batch test II, respectively). Both tests were performed under identical conditions. The PLA/P(3HB-co-4HB) blends were chopped into squares with a weight of approximately 0.3 mg. The biodegradation of PLA/P(3HB-co-4HB) blends was then performed in 2.5 L of static aerated lake water with an aeration rate of 40 mL L^{-1} . The temperature of the illumination incubator was maintained at $25\text{ }^\circ\text{C}$. The light/dark cycle was 12 h: 12 h with an intensity of 510 lux. Lake water from the grounds of Tongji University (Shanghai, China) was used for the biodegradation tests following sedimentation for 1 h to remove solid particles. Due to the metabolism of microorganisms within the original organic matter of the sample lake water, blanks without PLA/P(3HB-co-4HB) blends were used as a control in this study. Water samples were collected every 12 h, and the concentration of nitrite (ISO method 15923-1:2013), nitrous oxides (ISO method 15923-1:2013), nitrate (the difference between nitrous oxides and nitrite), ammonium (EPA method 350.1 Rev.2.0), and orthophosphate (EPA method 365.1, Rev. 2.0) were measured with an AQ2 analyzer (SEAL, UK). After 8 d of biodegradation for electrospun blends and 10.5 d of biodegradation for melt compounded blends, the blends were removed, washed with distilled water and dried to a constant weight at $80\text{ }^\circ\text{C}$ for characterization.

2.3.3 Scanning electron microscopy. SEM was performed to evaluate the morphology of the synthesized blends before and after degradation. Samples were coated with a thin layer of gold and then observed with a field emission scanning electron microscope S-520 (HITACHI, Japan) at an accelerating voltage of 20 kV. The diameter of the nano-fibers composing the electrospun blends was acquired from these images.

3. Results and Discussion

3.1 Characterization of PLA/P(3HB-co-4HB) blends

3.1.1 FT-IR spectra of PLA/P(3HB-co-4HB) blends. To assess the differences among PLA/P(3HB-co-4HB) blends, FT-IR spectra were analysed. There was little difference in the absorption positions of characteristic bonds between electrospun blends and melt compounded blends (Fig. 1), though synthesized melt compounded blends (Fig. 1b) exhibited more intensive absorption than synthesized electrospun blends (Fig. 1a). However, neat PLA and neat P(3HB-co-4HB) showed different peaks obviously. Although they exhibited similar absorption at approximately 1184 cm^{-1} , which corresponds to the -C-O- bond stretching vibration of the -CH-O- group, absorption corresponding to the asymmetric and symmetric deformation vibration of the -CH₃ group of neat PLA and neat P(3HB-co-4HB) was observed at approximately 1452 cm^{-1} and 1380 cm^{-1} , respectively. Neat PLA and neat P(3HB-co-4HB) also showed strong absorption at 1750 cm^{-1} and 1720 cm^{-1} , respectively, which corresponds to the asymmetric stretching vibration of the carbonyl group (-C=O). The absorption bands corresponding to the -C-O- bond stretching vibration of O=C-O- group were observed at 1085 cm^{-1} in neat PLA and at 1057 cm^{-1} in neat P(3HB-co-4HB). Moreover, the absorption bands corresponding to the asymmetric and symmetric stretching vibration of the -CH₃ group of neat PLA were observed at 2993 cm^{-1} and 2943 cm^{-1} , respectively, whereas those of neat P(3HB-co-4HB) were observed at 2975 cm^{-1} and 2933 cm^{-1} (not shown in Fig. 1). Blends with different ratios of PLA and P(3HB-co-4HB) shared similar absorption characteristics with neat PLA or P(3HB-co-4HB), depending on the content of the polyester, whereas red shifts of several absorption bands were observed with increasing P(3HB-co-4HB) content in the blends, and shoulder peaks of blends were also observed, indicating that P(3HB-co-4HB) and PLA were incompletely miscible in the synthesis processes.

3.1.2 Crystallinities of PLA/P(3HB-co-4HB) blends. Figs. 2a and b showed the XRD patterns of synthesized PLA/P(3HB-co-4HB) blends, which exhibited the crystallization of blends, and the crystallinity of the blends (Fig. 2c) was estimated based on them. The amorphous peaks of neat PLA were observed, indicating that neat PLA, by either the electrospinning process or the melt compounding process, was almost amorphous. Whereas neat P(3HB-co-4HB) was observed to be crystalline because of the peaks in the range of $2\theta = 12\text{--}30^\circ$, and the crystallinity of the blends was enhanced with increasing P(3HB-co-4HB) content. In addition, melt compounded PLA/P(3HB-co-4HB) blends exhibited greater crystallinity than electrospun PLA/P(3HB-co-4HB) blends, which may be ascribed to incomplete crystallization caused by rapid solvent evaporation during the electrospinning process.

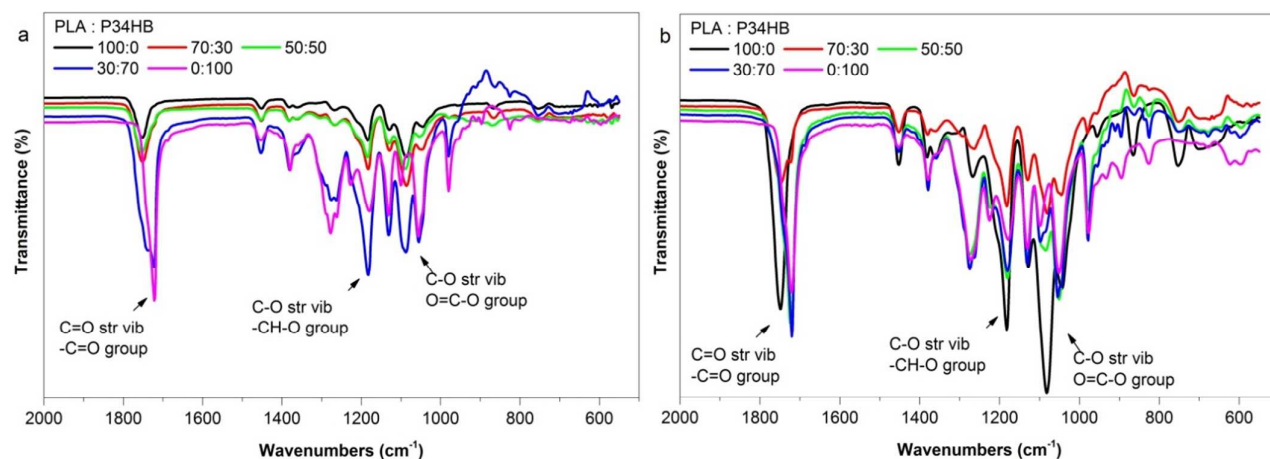


Fig. 1. FT-IR-ATR spectra of synthesized electrospun PLA/P(3HB-co-4HB) blends (a) and synthesized melt compounded PLA/P(3HB-co-4HB) blends (b).

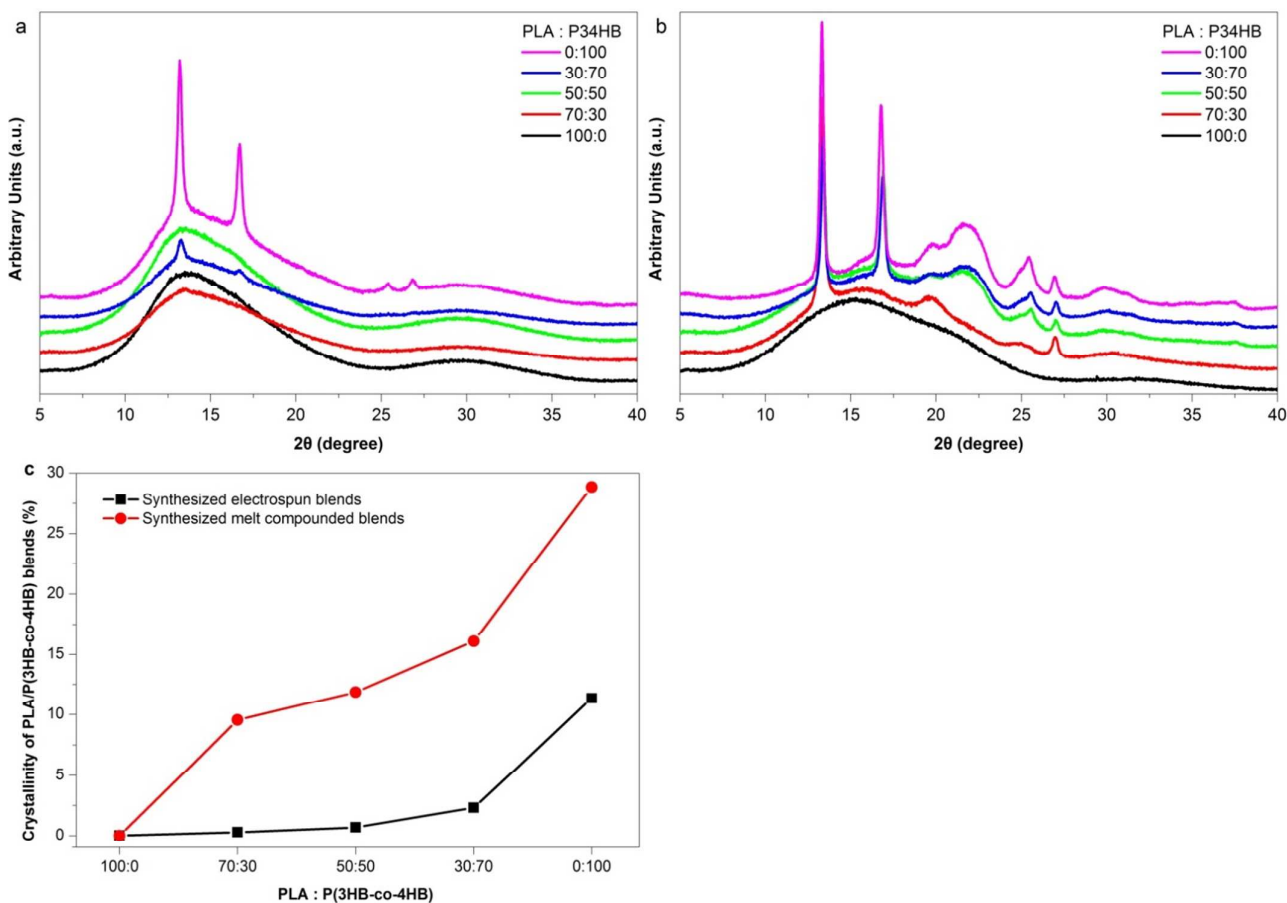


Fig. 2. XRD patterns of synthesized electrospun PLA/P(3HB-co-4HB) blends (a), synthesized melt compounded PLA/P(3HB-co-4HB) blends (b) and crystallinity of synthesized PLA/P(3HB-co-4HB) blends (c).

3.1.3 Micro-morphologies of PLA/P(3HB-co-4HB) blends.

Surface morphologies of PLA/P(3HB-co-4HB) blends are shown in Fig. 3. All electrospun blends displayed a large specific surface area with high porosity. Electrospun blends with 100

wt-% and 70 wt-% PLA blends exhibited poor electrospinning performance (indicated by the formation of beads), whereas electrospun blends with 50 wt-%, 30 wt-% and 0 wt-% PLA showed perfect morphologies and clear, fine fiber dispersion

with diameters ranging from 0.25 μm to 0.5 μm . In contrast, compact structures without pores were observed in melt compounded blends, resulting in relatively less specific surface area compared with electrospun blends. It should be noted

that all blends presented rough surfaces, which are favorable for the attachment of microorganisms to degrade the polyesters.

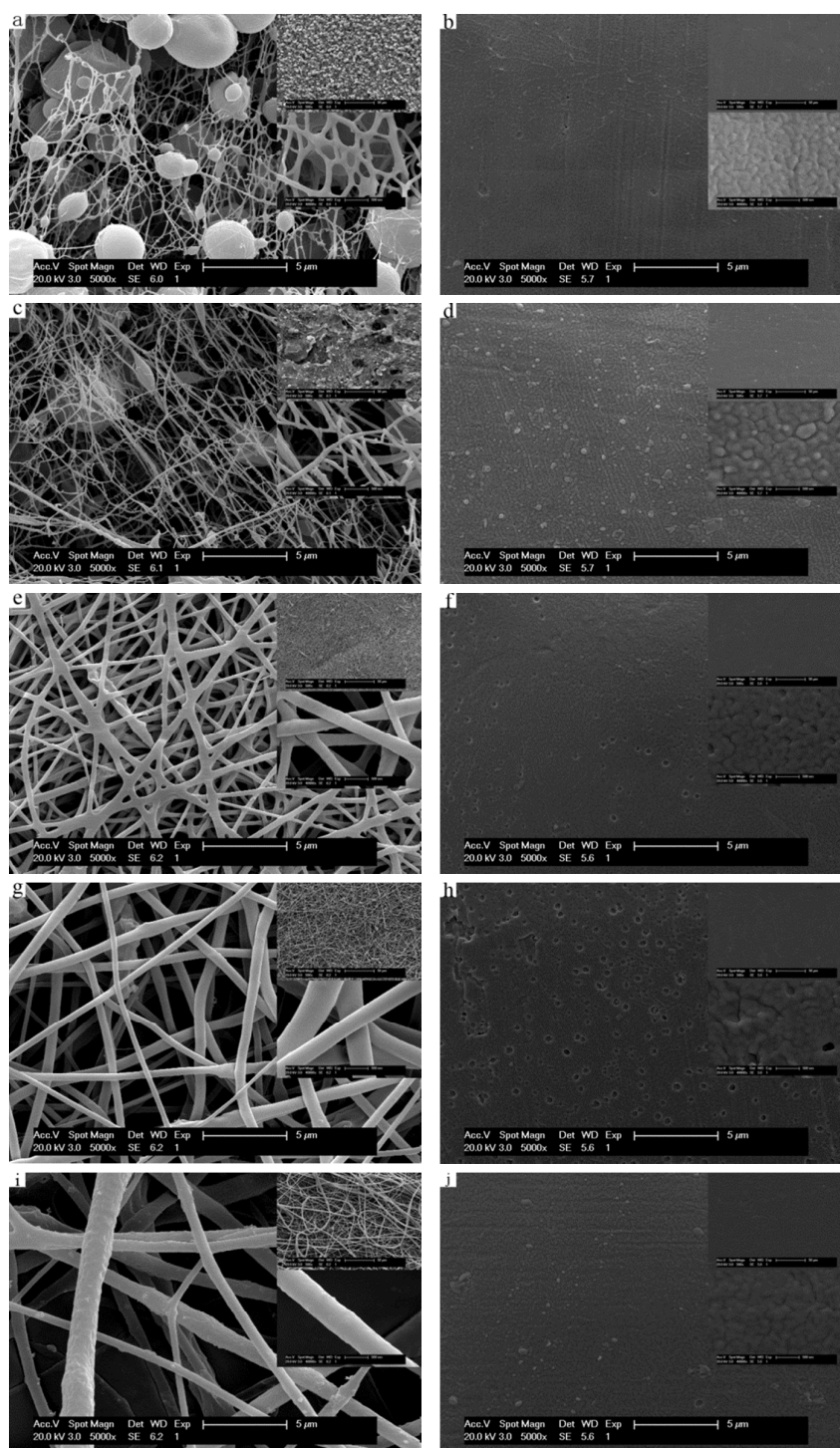


Fig. 3. SEM images of synthesized PLA/P(3HB-co-4HB) blends. The content of PLA in electrospun PLA/P(3HB-co-4HB) blends: (a) 100 wt-%, (c) 70 wt-%, (e) 50 wt-%, (g) 30 wt-% and (i) 0 wt-%. The content of PLA in melt compounded PLA/P(3HB-co-4HB) blends: (b) 100 wt-%, (d) 70 wt-%, (f) 50 wt-%, (h) 30 wt-% and (j) 0 wt-%.

3.2 Nutrient removal via biodegradation of PLA/P(3HB-co-4HB) blends in lake water

3.2.1 Removal of orthophosphate. The degradation of PLA and P(3HB-co-4HB) by microorganisms removed nitrogen and phosphorus from the lake water samples because nitrogen and phosphorus are essential elements in microbial metabolism. The results demonstrated that the removal of nitrogen and phosphorus from water was more effective when PLA/P(3HB-co-4HB) blends were present.

The removal of orthophosphates from lake water over time during the biodegradation of PLA/P(3HB-co-4HB) blends is plotted in Fig. 4. Controls were carried out under the same degradation conditions without the addition of degradable PLA/P(3HB-co-4HB) blends. The results showed that the concentration of orthophosphate in all lake water samples dropped dramatically within 12 hours, which might be ascribed to the assimilation of orthophosphate under aerobic conditions, and the concentration of orthophosphate in the batch test I and batch test II exhibited decreases of 59.3% - 86.4% and 77.8% - 92.6%, respectively. However, after a sharp decrease, a slight increase of orthophosphate in most water samples was observed before it finally started to decrease to almost zero. The observation might be due to the growth adaptation of microorganism after the abrupt assimilation of orthophosphate. Water samples with PLA/P(3HB-co-4HB) blends exhibited improved orthophosphate removal compared with controls; over time, the concentration of orthophosphate in water samples with PLA/P(3HB-co-4HB) blends decreased to approximately zero, whereas the concentration of orthophosphate in the controls did not decrease further. These results indicate that the removal of orthophosphate is promoted by the degradation of PLA/P(3HB-co-4HB) blends.

3.2.2 Removal of ammonium. The ammonium removal profiles of the lake water samples over time during the biodegradation

of PLA/P(3HB-co-4HB) blends are presented in Fig. 5. The rate of ammonium removal can be calculated from the slope of ammonium concentration plotted against time. All water samples displayed complete removal of ammonium but at different rates. The slowest rate of removal of ammonium was observed in the blanks, suggesting that ammonium removal was promoted by the degradation of PLA/P(3HB-co-4HB) blends. Water samples with neat electrospun P(3HB-co-4HB) showed the highest rate of ammonium removal, and the concentration of ammonium decreased from 0.5536 mg N/L to zero within 1.5 days. The concentration of ammonium in water samples with neat electrospun PLA decreased from 0.5536 mg N/L to zero within 4.5 days, indicating that the removal of ammonium by enzymolysis of P(3HB-co-4HB) was greater than the removal of ammonium by hydrolysis of PLA. Moreover, the removal rates of ammonium increased with an increase in P(3HB-co-4HB) content of electrospun blends, with the exception of the 70 wt-% PLA blend. Water samples with 70 wt-% PLA showed the lowest rate of ammonium removal among the batch I tests, and it took approximately 6 days for the concentration of ammonium to decrease from 0.5536 mg N/L to zero.

Similar rates of degradation and ammonium removal were observed in water samples with melt compounded blends. Ammonium removal increased with an increase in P(3HB-co-4HB) content, with the exception of the blend with 50 wt-% PLA. Water samples with neat melt compounded PLA showed the lowest ammonium removal rate among the batch II tests, and it took approximately 5.5 days for the concentration of ammonium to decrease from 0.4365 mg N/L to zero. Water samples with the melt compounded blend containing 50 wt-% PLA displayed the most rapid ammonium removal among the batch II tests, and the concentration of ammonium decreased from 0.4365 mg N/L to zero in 2.5 days.

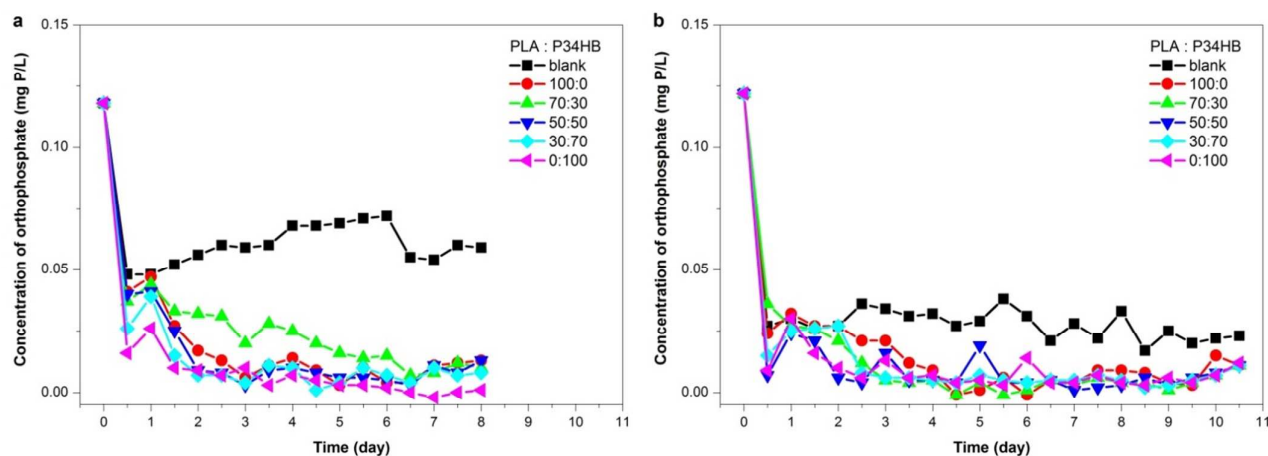


Fig. 4. Orthophosphate removal profiles of lake water as a function of time during the biodegradation of electrospun PLA/P(3HB-co-4HB) blends (a) and melt compounded PLA/P(3HB-co-4HB) blends (b).

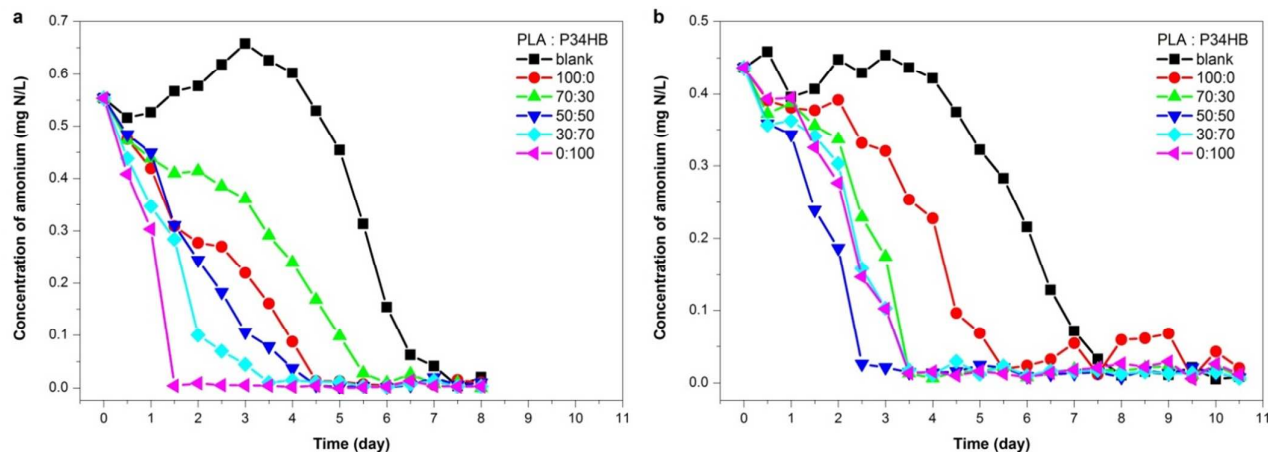


Fig. 5. Ammonium removal profiles of lake water as a function of time during the biodegradation of electrospun PLA/P(3HB-co-4HB) blends (a) and melt compounded PLA/P(3HB-co-4HB) blends (b).

3.2.3 Removal of total inorganic nitrogen and nitrous oxides.

Total inorganic nitrogen was calculated as the sum of ammonium, nitrate and nitrite. The removal of total inorganic nitrogen from lake water is plotted over time in Figs. 6a and b, and showed a removal pattern similar to ammonium. The concentration of total inorganic nitrogen in water samples with PLA/P(3HB-co-4HB) blends decreased over time. The concentration of total inorganic nitrogen in batch test I and batch test II decreased by 9.1% - 49.5% and 19.8% - 52.9%, respectively, within 8 days. In contrast, the concentration of total inorganic nitrogen in the blank tests was variable but high, indicating that the degradation of PLA and P(3HB-co-4HB) promoted the removal of nitrogen from lake water. As shown in Fig. 6, the removal of nitrate in blank tests was rarely observed, whereas nitrite accumulated dramatically after a slight rise. The concentration of nitrite in blank tests reached approximately 0.81 mg N/L and 0.34 mg N/L for electrospun and melt compounded blends, respectively. These results revealed that nitrous oxides were not reduced in the blank tests, thus causing the accumulation of nitrite. In contrast, nitrate removal and therefore minimal nitrite accumulation were observed during the degradation of PLA/P(3HB-co-4HB) blends, indicating that the degradation of PLA/P(3HB-co-4HB) blends facilitated the removal of nitrous oxides from water samples.

3.3 Analysis of nutrient removal promoted by the degradation of PLA/P(3HB-co-4HB) blends

Enhanced nutrient removal was observed during the degradation of PLA/P(3HB-co-4HB) blends in lake water samples. Orthophosphate and ammonium were almost completely removed in water samples with PLA/P(3HB-co-4HB) blends, and the concentration of total inorganic nitrogen and nitrate decreased over time. The accumulation of nitrite was inhibited by the degradation of PLA/P(3HB-co-4HB) blends. Nitrate is produced by the nitrification of ammonium,

and nitrate is subsequently reduced to nitrite and gaseous substances. It is proposed that the degradation of PLA/P(3HB-co-4HB) blends provided the carbon sources that supported the denitrification of nitrous oxides, and the denitrification of nitrous oxides accelerated the nitrification of ammonium. Simultaneously, the degradation of PLA/P(3HB-co-4HB) blends supplied carbon sources for assimilation by microorganisms, and the orthophosphate was assimilated into cell components as the microorganisms proliferated. Consumption of the degradation products of PLA/P(3HB-co-4HB) blends further promoted the degradation of PLA/P(3HB-co-4HB) blends.

FT-IR spectra were used to assess the degradation of PLA/P(3HB-co-4HB) blends (Fig. 7). Following degradation in lake water, the -C=O band intensities of PLA/P(3HB-co-4HB) blends decreased, indicating chain scission of blends during degradation. Broader absorption and narrower shoulder bands corresponding to the carbonyl group were noted in degraded blends, which were related to the loss of miscibility between PLA and P(3HB-co-4HB)²³. Weaker -C-O- bands associated with the amorphous phase of samples were observed, and upward bends emerged in the 950-500 cm⁻¹ region following degradation, which might be ascribed to the degradation of the amorphous phase of the samples²³. Decreased absorption corresponding to the -CH₃ group was observed, providing further support for the degradation of PLA/P(3HB-co-4HB) blends in lake water samples over time.

The degradation of polyesters is influenced by factors such as illumination, temperature, microorganisms, surface morphology, crystallinity and polyester composition. It is reported that PLA and P(3HB-co-4HB) are degraded via different mechanisms^{16, 22, 26}. The degradation of PLA in biological environments occurs in two main stages: hydrolysis and enzymolysis. Ester linkages are broken by hydrolysis, and the resulting low molecular weight products are assimilated by fungi or bacteria. Because the degradation of PLA typically starts with hydrolysis, water absorption plays an important role in the degradation process. Therefore, the hydrolysis of

PLA is associated with the porosity and specific surface area of blends. In contrast, P(3HB-co-4HB) is degraded by microbial erosion, influenced heavily by crystallinity and surface morphology²⁸. The degradation starts in the amorphous region of P(3HB-co-4HB) following depolymerase bonding to the crystalline area, known as crystalline-induced biodegradation¹⁵,

²⁹. In this study, environmental conditions, i.e., illumination, microorganisms and temperature, were held constant. Thus, the degradation of PLA/ P(3HB-co-4HB) blends depended largely on crystallinity, surface morphology and polyester composition.

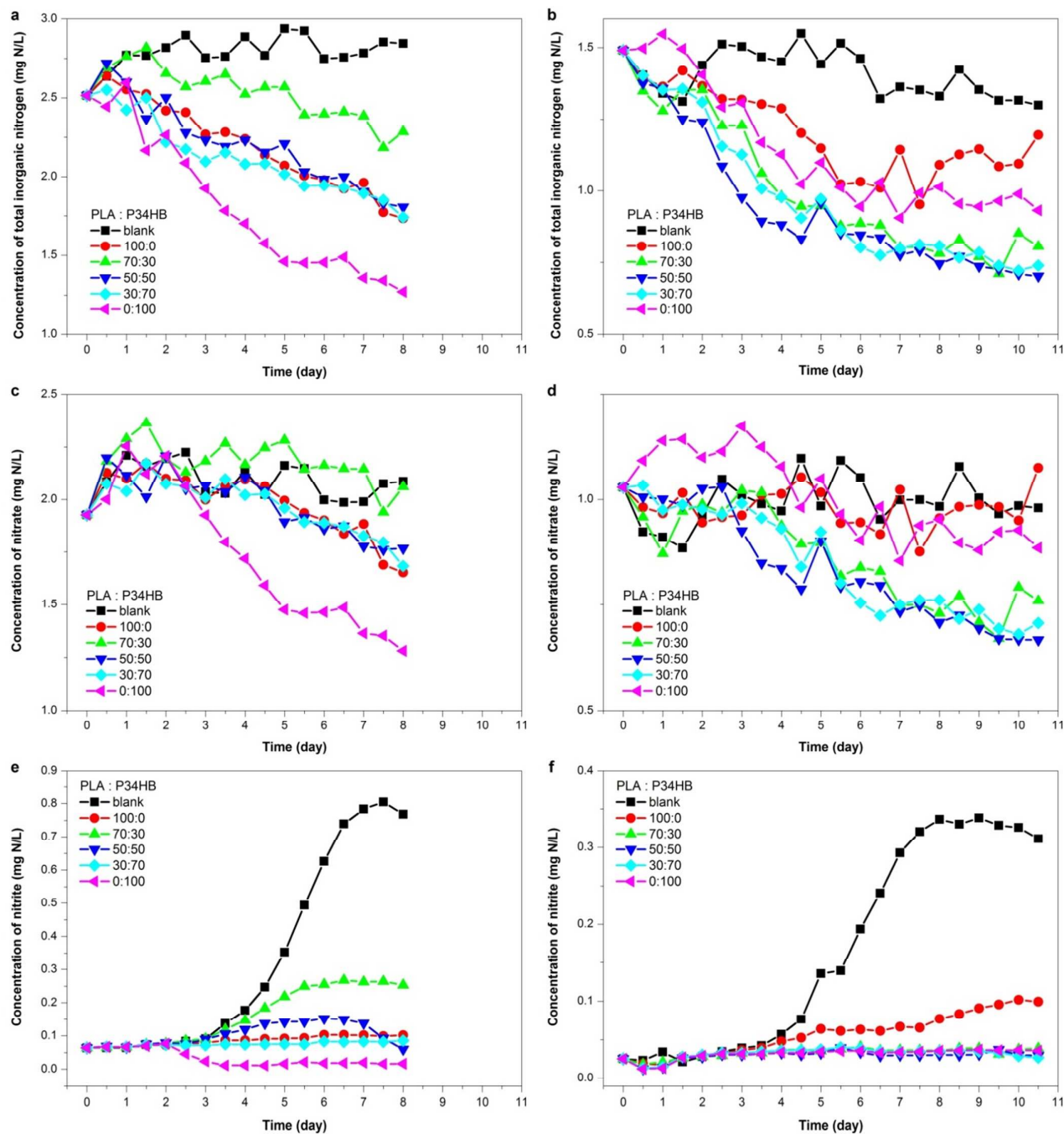


Fig. 6. Total inorganic nitrogen (a), nitrate (c) and nitrite (e) removal profiles of lake water as a function of time during the biodegradation of electrospun PLA/P(3HB-co-4HB) blends; total inorganic nitrogen (b), nitrate (d) and nitrite (f) removal profiles of lake water as a function of time during the biodegradation of melt compounded PLA/P(3HB-co-4HB) blends.

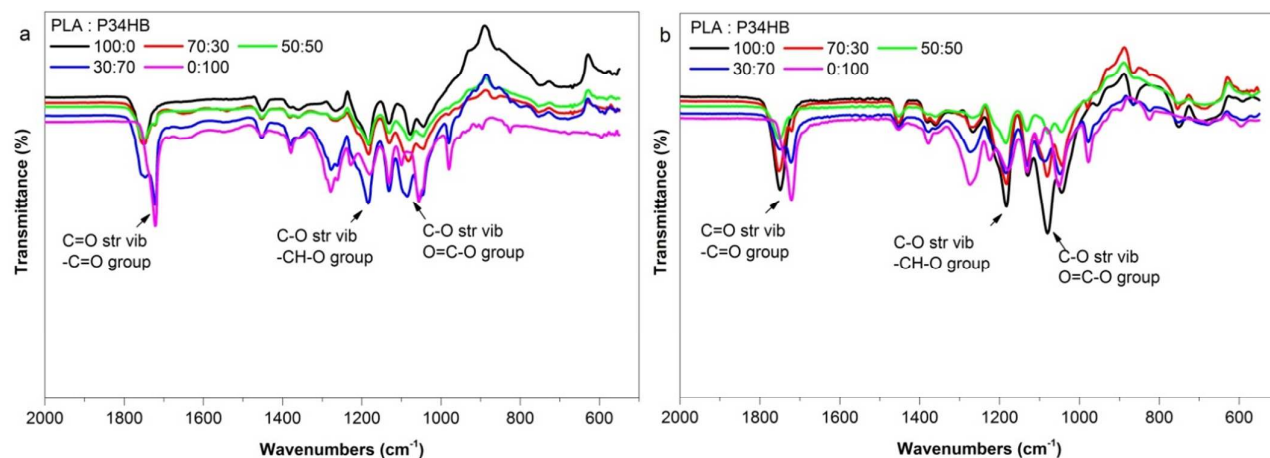


Fig. 7. FT-IR-ATR spectra of electrospun PLA/P(3HB-co-4HB) blends after degradation (a) and melt compounded PLA/P(3HB-co-4HB) blends after degradation (b).

To validate the biodegradation of the PLA/P(3HB-co-4HB) blends and clarify the reason for biodegradation, X-ray diffraction was used to analyse the crystallinity of the blends. XRD patterns of PLA/P(3HB-co-4HB) blends following degradation are presented in Figs. 8a and b; neat P(3HB-co-4HB) is not presented because it was difficult to collect the pasted sample for detection. The crystallinity of PLA/P(3HB-co-4HB) blends following degradation were presented in Fig. 8c. Increases in the crystallinity of almost all samples was observed following degradation, which may be attributed to the preferential degradation of amorphous phases of the PLA/P(3HB-co-4HB) blends and the structural rearrangement of polyesters during degradation. Peaks of neat PLA after degradation were observed in the range of $2\theta = 12-30^\circ$, indicating the crystallization of PLA during degradation. However, the peaks and crystallinity of neat P(3HB-co-4HB) remained nearly unchanged, suggesting that the crystallization of PLA is essential to the increased of crystallinity of samples during biodegradation.

The surface morphologies of PLA/P(3HB-co-4HB) blends after degradation are presented in Fig. 9. Electrospun blends containing PLA had thicker fiber diameters after degradation, which might be ascribed to the swelling of PLA during hydrolysis. Neat electrospun PLA displayed a greater increase in fiber diameter than electrospun blend with 70 wt-% PLA, indicating that the swelling of fibers is enhanced by increasing PLA content. In contrast, the fiber diameter of neat P(3HB-co-4HB) remained almost unchanged, supporting the suggestion that the swelling of blends is related to the hydrolysis of PLA. Conglomerations of electrospun blends containing PLA were observed, which can be explained by the rearrangement of ester bonds and the crystallization of PLA following degradation, as inferred above. The small fiber diameter and the beads of neat electrospun PLA illustrated in Fig. 3 and Fig. 9 improved the contact of PLA with the aqueous phase, resulting in rapid hydrolysis of amorphous PLA, and therefore rapid removal of ammonium from the water samples with neat electrospun PLA. However, in water samples with electrospun

blends containing 70 wt-% PLA, a slower removal of ammonium was observed because P(3HB-co-4HB) is wrapped in a PLA-rich phase and cannot make sufficient contact with enzymes. Thus, a lower PLA content and an insufficient degradation domain for P(3HB-co-4HB) led to the slowest degradation in electrospun blend with 70 wt-% PLA, as well as the slowest removal of ammonium from water sample. Moreover, the fibers of the electrospun blends containing P(3HB-co-4HB) became coarse as a result of degradation, which was attributed to the degradation of P(3HB-co-4HB).

In comparison, the melt compounded blends presented a different morphology following degradation. Coarser surfaces and caverns were observed on melt compounded blends with 0 wt-%, 30 wt-% and 50 wt-% PLA after degradation, whereas the surface morphology of melt compounded blends with 70 wt-% and 100 wt-% PLA remained virtually unchanged, indicating more rapid degradation of P(3HB-co-4HB) compared with PLA. Following degradation, microspheres were observed in melt compounded blend with 30 wt-% PLA, suggesting incomplete miscibility between the two polyesters. This observation could be explained by the wraparound effect¹⁶ of P(3HB-co-4HB) during the melt compounding process. Because PLA was wrapped in a P(3HB-co-4HB)-rich phase and the hydrolysis of PLA was inhibited, microspheres formed during the biodegradation of P(3HB-co-4HB). Melt compounded blend with 50 wt-% PLA exhibited the largest pore size after degradation, and water samples with melt compounded blend containing 50 wt-% PLA displayed the most rapid removal of ammonium. This observation may be ascribed to the equal compounding ratio of PLA and P(3HB-co-4HB) in the blend, due to the incomplete miscibility of blends, producing the largest specific surface area among the blends. The two-phase nature of blends containing an equal compounding ratio of PLA and P(3HB-co-4HB) facilitates water absorption and enzyme diffusion from the surface to the inside of the blends^{7, 26}; as a result, the degradation of P(3HB-co-4HB) and hydrolysis of PLA are improved.

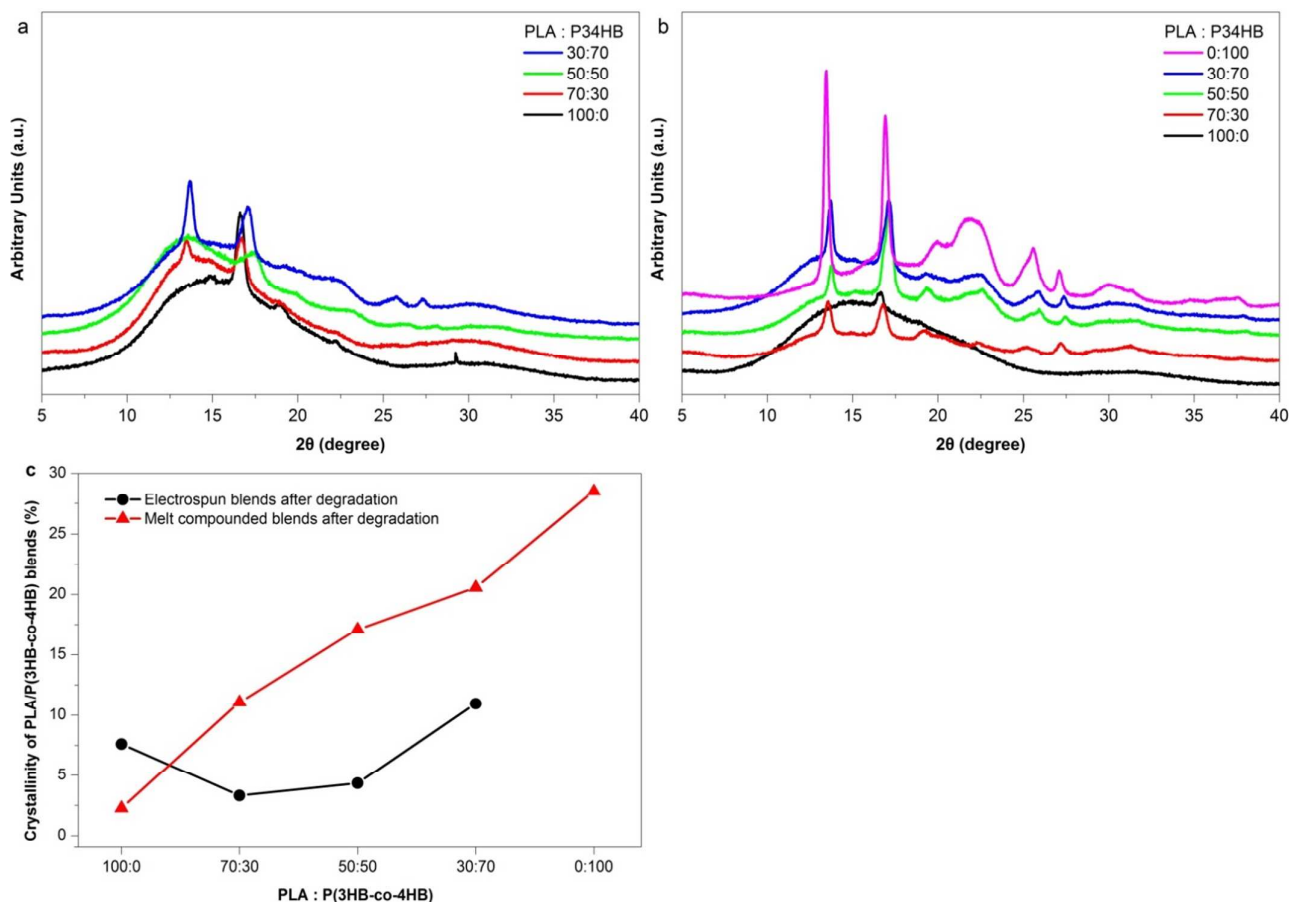


Fig. 8. XRD patterns of electrospun PLA/P(3HB-co-4HB) blends after degradation (a), melt compounded PLA/P(3HB-co-4HB) blends after degradation (b) and crystallinity of PLA/P(3HB-co-4HB) blends after degradation (c).

It is conjectured that the degradation of P(3HB-co-4HB), and thus nutrient removal, is predominantly restricted by crystallinity when the crystallinities of the blends are below a particular level. As discussed, neat P(3HB-co-4HB) shows greater crystallinity than neat PLA, and the crystallinity of blends is improved with a rising P(3HB-co-4HB) content. Thus, nutrients removal, such as ammonium removal, are enhanced by a rising P(3HB-co-4HB) content, with the exception of electrospun blends with 70 wt-% PLA and melt compounded blends with 50 wt-% PLA. At the same time, degradation of P(3HB-co-4HB) is rapid compared with PLA. Moreover, melt compounded blends containing both PLA and P(3HB-co-4HB) displayed more rapid ammonium removal than electrospinning blends because melt compounded blends showed higher crystallinity, supporting the proposal that crystallinity drives degradation and nutrient removal. However, the specific surface area limits the degradation of P(3HB-co-4HB) when the

crystallinity of blends is sufficient to provide enzyme-binding sites for degradation. Water samples with neat electrospun PLA and neat electrospun P(3HB-co-4HB) showed faster ammonium removal than water samples with melt compounded blends, demonstrating that the crystallinity of neat electrospun P(3HB-co-4HB) provides sufficient enzyme-binding sites for the enzymolysis of P(3HB-co-4HB). This result is ascribed to the larger specific surface areas engendered by the electrospinning process, which improved the enzymolysis of P(3HB-co-4HB) and the hydrolysis of PLA.

Therefore, the application of biodegradable PLA/P(3HB-co-4HB) blends for nutrient removal from lake water becomes a reasonable and innovative option. Melt compounded blend with 50% PLA is considered to be the optimal choice for nutrient removal from lake water because the electrospinning process is expensive and without notable superiority in nutrient removal.

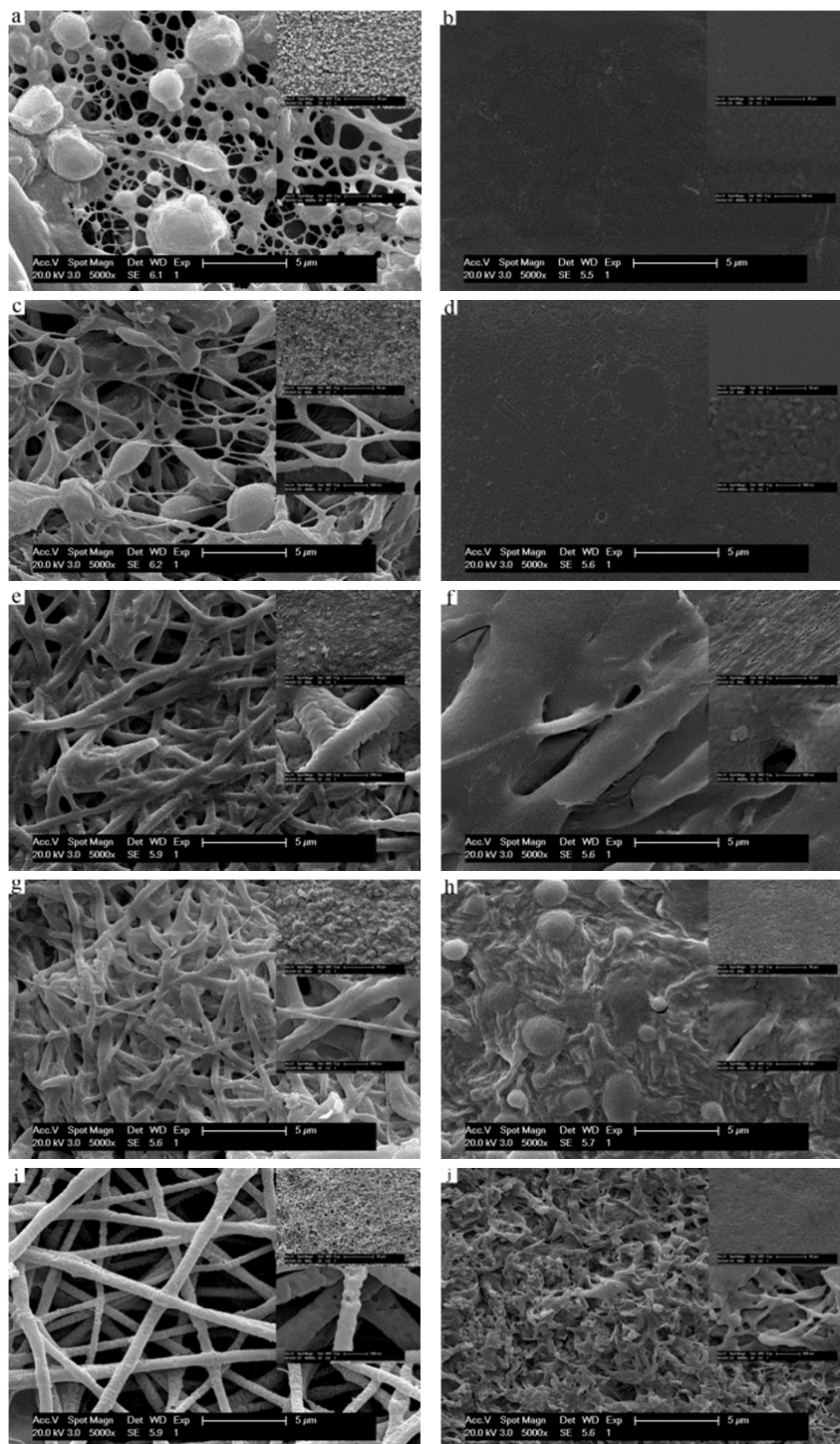


Fig. 9. SEM images of PLA/P(3HB-co-4HB) blends after degradation. The content of PLA in electrospun PLA/P(3HB-co-4HB) blends: (a) 100 wt-%, (c) 70 wt-%, (e) 50 wt-%, (g) 30 wt-% and (i) 0 wt-%. The content of PLA in melt compounded PLA/P(3HB-co-4HB) blends: (b) 100 wt-%, (d) 70 wt-%, (f) 50 wt-%, (h) 30 wt-% and (j) 0 wt-%.

4. Conclusions

Biodegradable blends with different ratios of PLA and P(3HB-co-4HB) were applied for the removal of nutrients from lake water. Nutrient removal from lake water was accelerated by the degradation of PLA/P(3HB-co-4HB) blends.

Orthophosphate and ammonium were almost completely removed from water samples containing PLA/P(3HB-co-4HB) blends. The concentrations of total inorganic nitrogen and nitrate decreased over time, and the accumulation of nitrite was inhibited. The degradation of PLA/P(3HB-co-4HB) blends was influenced by crystallinity, surface morphology and the composition of blends. Given their favorable properties and high efficiency of nutrient removal, shaped insoluble PLA/P(3HB-co-4HB) blends with 50 wt-% PLA have a potential application as slow-release carbon sources for nutrient removal from lake water.

Acknowledgements

The authors are grateful for the support from the State Key Laboratory of Pollution Control and Resource Reuse Foundation (Tongji University) (No. PCRRY11016).

References

1. D. W. Schindler, *Proceedings of the Royal Society B-Biological Sciences*, 2012, **279**, 4322-4333.
2. X.-N. Li, H.-L. Song, W. Li, X.-W. Lu and O. Nishimura, *Ecological Engineering*, 2010, **36**, 382-390.
3. Y. Zhao, Z. Yang, X. Xia and F. Wang, *Water Research*, 2012, **46**, 5635-5644.
4. F. Pietrini, M. A. Iannelli, S. Pasqualini and A. Massacci, *Plant Physiology*, 2003, **133**, 829-837.
5. B. R. Silliman and M. D. Bertness, *Conservation Biology*, 2004, **18**, 1424-1434.
6. N. Fu, J. Xie, G. Li, X. Shao, S. Shi, S. Lin, S. Deng, K. Sun and Y. Lin, *Rsc Advances*, 2015, **5**, 21572-21579.
7. Z. Chen, S. Cheng and K. Xu, *Biomaterials*, 2009, **30**, 2219-2230.
8. A. S. Asran, K. Razghandi, N. Aggarwal, G. H. Michler and T. Groth, *Biomacromolecules*, 2010, **11**, 3413-3421.
9. E. Hablot, S. Dharmalingam, D. G. Hayes, L. C. Wadsworth, C. Blazy and R. Narayan, *Journal of Polymers and the Environment*, 2014, **22**, 417-429.
10. M. P. Arrieta, J. Lopez, A. Hernandez and E. Rayon, *European Polymer Journal*, 2014, **50**, 255-270.
11. M. Kwiecien, G. Adamus and M. Kowalczyk, *Biomacromolecules*, 2013, **14**, 1181-1188.
12. K. Bubel, Y. Zhang, Y. Assem, S. Agarwal and A. Greiner, *Macromolecules*, 2013, **46**, 7034-7042.
13. K. Kim, M. Yu, X. H. Zong, J. Chiu, D. F. Fang, Y. S. Seo, B. S. Hsiao, B. Chu and M. Hadjiargyrou, *Biomaterials*, 2003, **24**, 4977-4985.
14. Y. Ding, J. A. Roether, A. R. Boccaccini and D. W. Schubert, *European Polymer Journal*, 2014, **55**, 222-234.
15. H. Zhao, Y. Bian, Y. Li, Q. Dong, C. Han and L. Dong, *Journal of Materials Chemistry A*, 2014, **2**, 8881-8892.
16. D. Ju, L. Han, J. Bian, Z. Guo, F. Li, S. Chen and L. Dong, *Rsc Advances*, 2015, **5**, 5474-5483.
17. K. Odelius, A. Hoglund, S. Kumar, M. Hakkarainen, A. K. Ghosh, N. Bhatnagar and A.-C. Albertsson, *Biomacromolecules*, 2011, **12**, 1250-1258.
18. T. G. Volova, M. I. Gladyshev, M. Y. Trusova and N. O. Zhila, *Polymer Degradation and Stability*, 2007, **92**, 580-586.
19. H. Tsuji and K. Suzuyoshi, *Polymer Degradation and Stability*, 2002, **75**, 347-355.
20. H. Tsuji and K. Suzuyoshi, *Polymer Degradation and Stability*, 2002, **75**, 357-365.
21. H. Tsuji and K. Suzuyoshi, *Journal of Applied Polymer Science*, 2003, **90**, 587-593.
22. Y.-X. Weng, L. Wang, M. Zhang, X.-L. Wang and Y.-Z. Wang, *Polymer Testing*, 2013, **32**, 60-70.
23. M. P. Arrieta, J. Lopez, E. Rayon and A. Jimenez, *Polymer Degradation and Stability*, 2014, **108**, 307-318.
24. A. Sodergard and M. Stolt, *Progress in Polymer Science*, 2002, **27**, 1123-1163.
25. S. Taguchi, M. Yamadaa, K. i. Matsumoto, K. Tajima, Y. Satoh, M. Munekata, K. Ohno, K. Kohda, T. Shimamura, H. Kambe and S. Obata, *Proceedings of the National Academy of Sciences of the United States of America*, 2008, **105**, 17323-17327.
26. I. Arrnentano, N. Bitinis, E. Fortunati, S. Mattioli, N. Rescignano, R. Verdejo, M. A. Lopez-Manchado and J. M. Kenny, *Progress in Polymer Science*, 2013, **38**, 1720-1747.
27. Y. Bian, C. Han, L. Han, H. Lin, H. Zhang, J. Bian and L. Dong, *Rsc Advances*, 2014, **4**, 41722-41733.
28. K. Sudesh, H. Abe and Y. Doi, *Progress in Polymer Science*, 2000, **25**, 1503-1555.
29. Z. Li, H. Lin, N. Ishii, G.-Q. Chen and Y. Inoue, *Polymer Degradation and Stability*, 2007, **92**, 1708-1714.

Abstract:

Shaped insoluble PLA/P(3HB-co-4HB) blends were applied as slow-release carbon sources to promote the removal of nutrients and facilitate the control of eutrophication in lake water. Various weight ratios of PLA/P(3HB-co-4HB) blends were prepared by electrospinning and melt compounding processes and were added to static aerated lake water. The properties of the blends and nutrient removal from lake water were characterized. The results demonstrated that nutrient removal was enhanced by degradation of PLA/P(3HB-co-4HB) blends, and the consumption of degradation products further promoted the degradation of blends. The orthophosphate concentrations of water samples with electrospun and melt compounded blends exhibited decreases of 59.3% - 86.4% and 77.8% - 92.6%, respectively, within 12 hours and decreased to approximately zero over time. Ammonium was completely removed within 1.5 - 6.5 days and 2.5 - 5.5 days from water samples with electrospun and melt compounded blends, respectively. Inhibition of nitrite accumulation was observed, and the total inorganic nitrogen content decreased by 9.1% - 49.5% and 19.8% - 52.9% within 8 days in water samples with electrospun and melt compounded blends, respectively. Thus, PLA/P(3HB-co-4HB) blends are potentially useful as slow-release carbon sources for nutrient removal from lake water. Moreover, Fourier transform infrared spectroscopy (FTIR), wide-range X-ray diffraction (XRD) and scanning electron microscopy (SEM) were used to characterize the degradation of PLA/P(3HB-co-4HB) blends, and the results showed that the degradation of PLA/P(3HB-co-4HB) blends is closely related to the crystallinity, surface morphology and composition of blends. Given the blends' favorable properties and high efficiency of nutrient removal, PLA/P(3HB-co-4HB) blends are potentially useful as slow-release carbon sources for nutrient removal from lake water. Melt compounded blends with 50 wt-% PLA are considered to be the optimal choice for this application.

